Supporting Information

Hydrothermal direct synthesis of polyaniline, graphene/polyaniline and N-doped graphene/polyaniline hydrogels for high performance flexible supercapacitors

Yubo Zou,[a] Zhicheng Zhang,[a] Wenbin Zhong,*[a] Wantai Yang[b]

[a] College of Materials Science and Engineering, Hunan University, Changsha, 410082, P. R. China.

[b] Department of Polymer Science, Beijing University of Chemical Technology, Beijing, 100029, P. R. China.

*Corresponding Author: wbzhong@hnu.edu.cn

Fig. S1 Photograph of the soluble PANI dispersion.

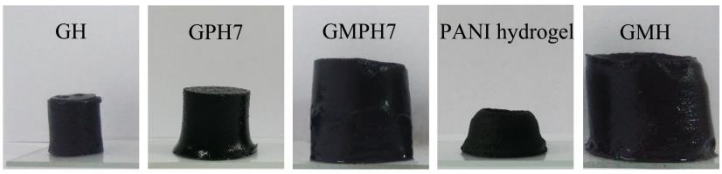

Fig. S2 Photographs of the PANI/graphene hydrogels with different components.

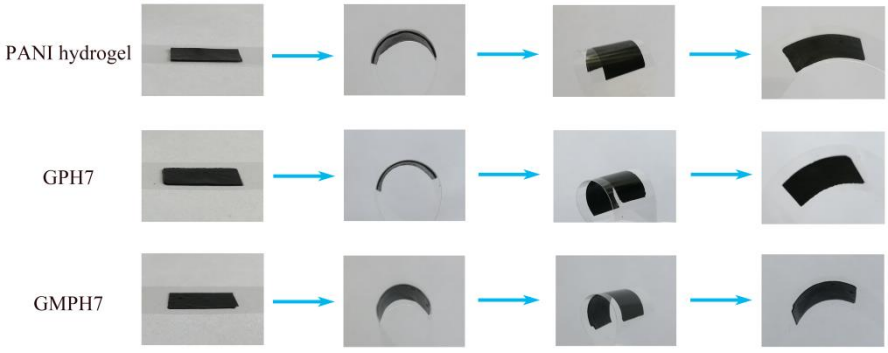

Fig. S3 Photographs of PANI hydrogel, GPH7 and GMPH7 slices (~0.1 mm in the thickness) under different bending angles.

The hydrogels were cut into the slices (~2 mm in the thickness) and then pressed under ~0.1 MPa to obtain the slices with ~0.1 mm in thickness. The as-prepared PANI hydrogel, GPH7 and GMPH7 thin slices can be bent at various angles and returned to the original state, implying good flexibility.

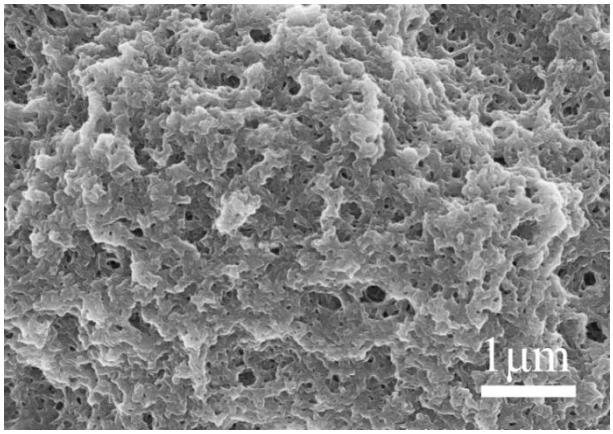

Fig. S4 SEM image of PANI synthesized without hydrothermal progress.

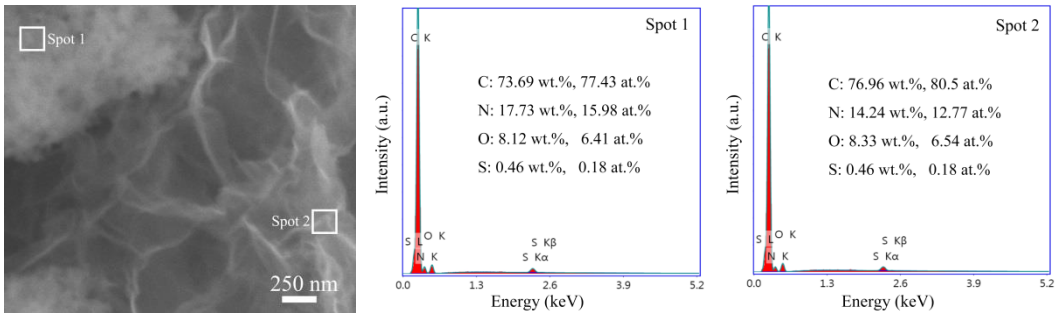

Fig. S5 SEM-EDS images of GMPH7.

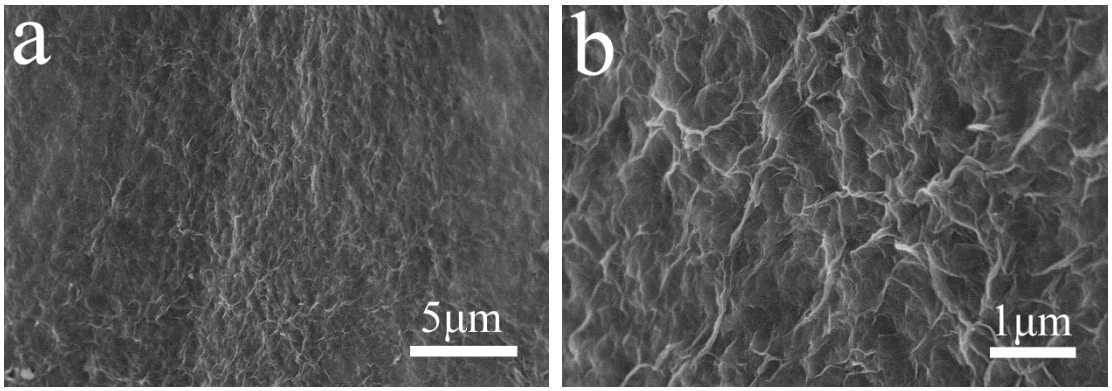

Fig. S6 SEM images of GMH.

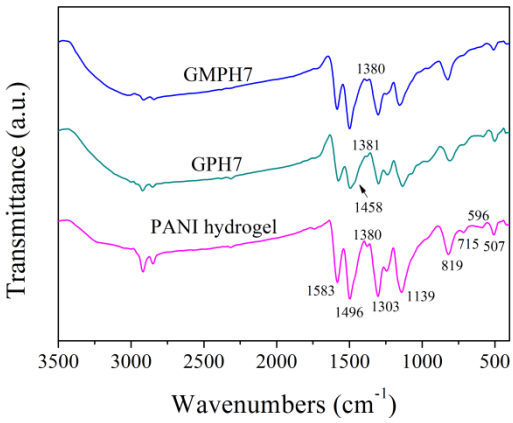

Fig. S7 FT-IR spectra of as-prepared PANI hydrogel, GPH7 and GMPH7.

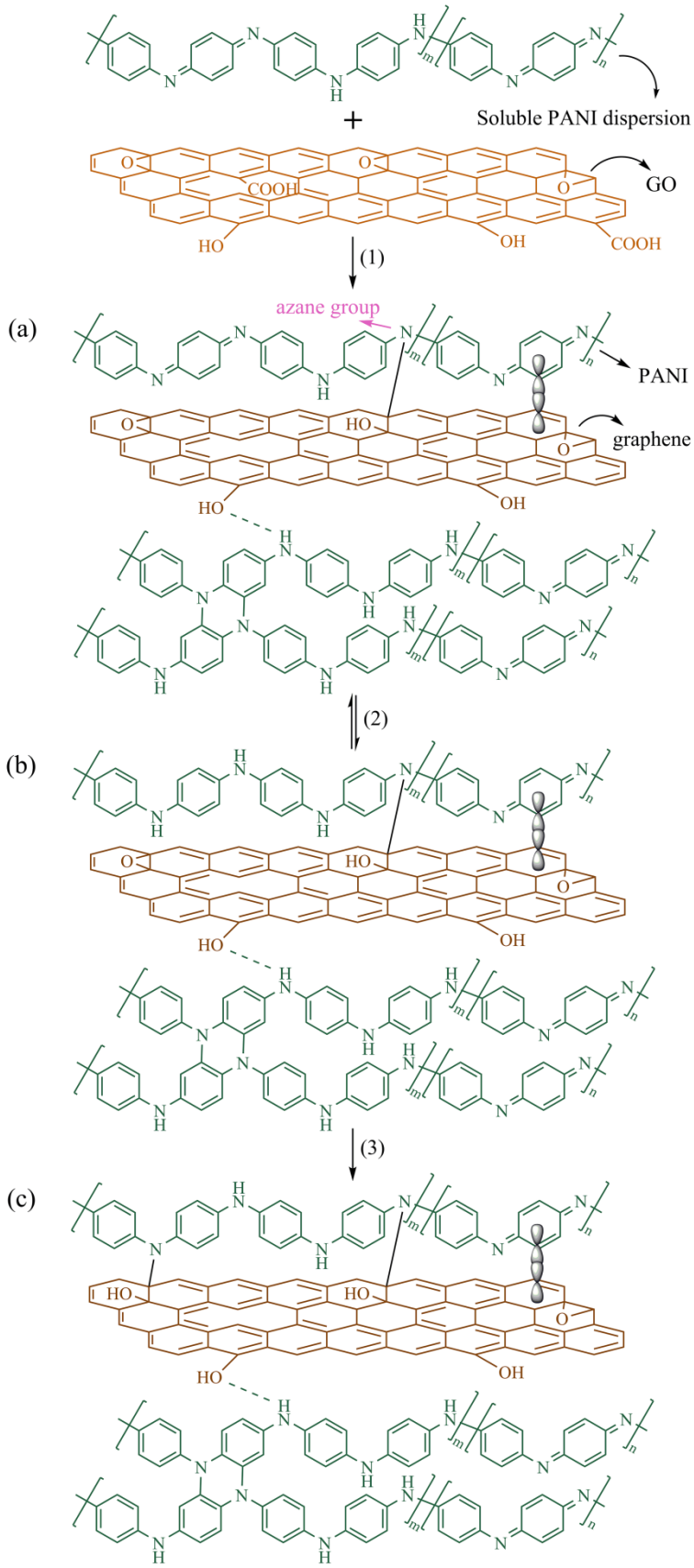

Fig. S8 The evolution of GPH7: (a) The product-1 obtained through (1) the epoxy ring-opening

reaction of imine groups in PANI chains and oxygen groups in GO; (b) The product-2 obtained through (2) the transformation from emeraldine form (a) to leucoemeraldine form in “m” unit; (c) The product-3 (GPH7) obtained through (3) the epoxy ring-opening reaction of imine group in PANI chains and oxygen group in GO.

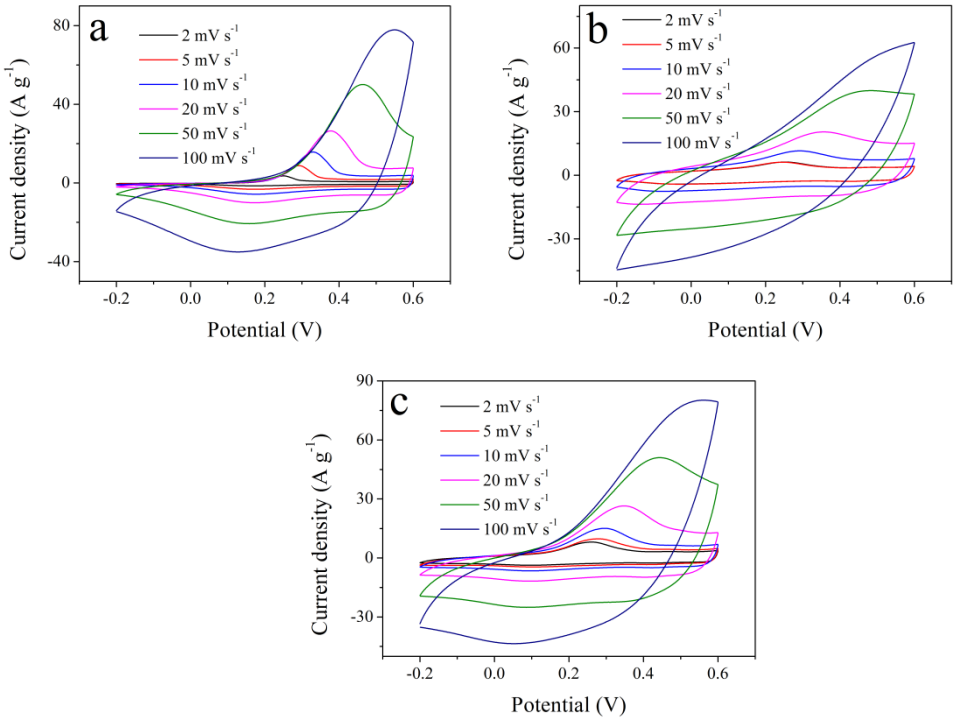

Fig. S9 CV curves of (a) PANI hydrogel, (b) GPH7 and (c) GMPH7 at different scan rates of 2, 5, 10, 20, 50 and 100 mV s^{-1}.

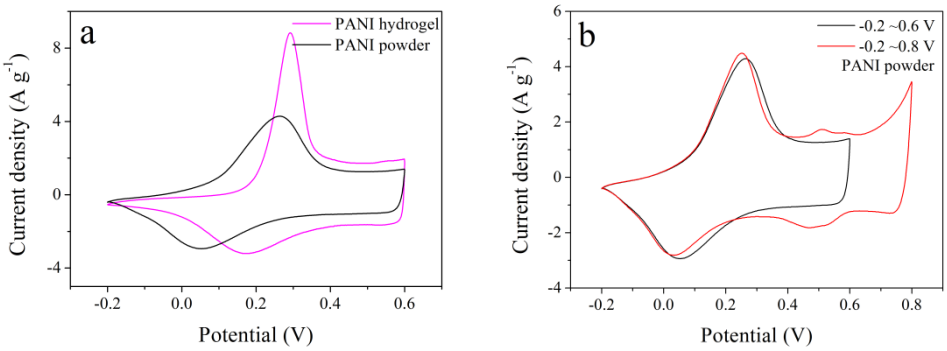

Fig. S10 The CV curve at the scan rate of 5 mV s^{-1} for (a) PANI hydrogel and PANI powder without hydrothermal process under a potential range of –0.2 to 0.6 V; (b) PANI powder under different potential ranges (black line: –0.2 to 0.6 V, red line: –0.2 to 0.8 V).

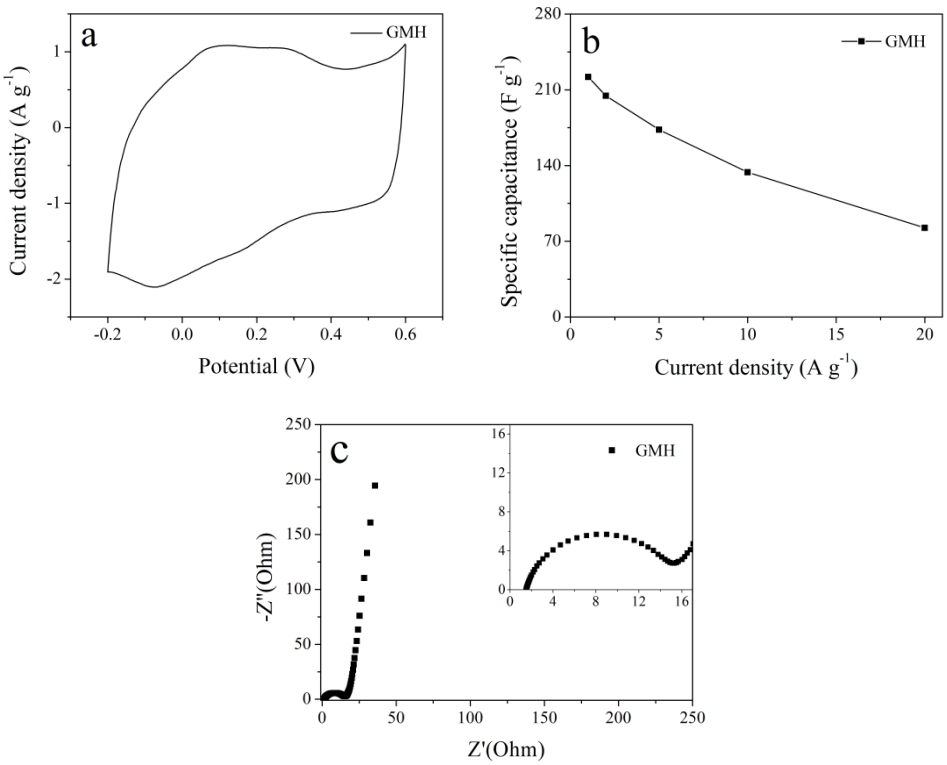

Fig. S11 (a) The CV curves at the scan rate of 5 mV s^{-1}, (b) Specific capacitance at different current densities and (c) Nyquist plots for GMH.

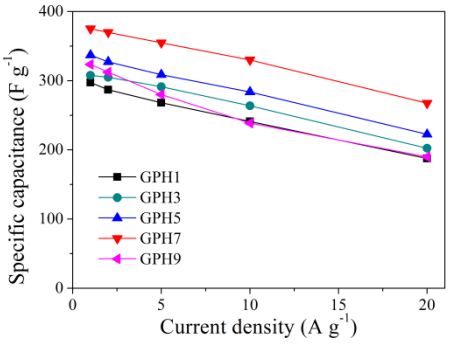

Fig. S12 The specific capacitance of GPH1, GPH3, GPH5, GPH7 and GPH9 at different current densities.

From Fig. S10, it was found that the specific capacitance was gradually increased as the mass ratio of PANI/GO increased from 1 to 7. The largest specific capacitance of GPH7 is 375 F g^{-1} at 1 A g^{-1}. However, the specific capacitance was decreased as the mass ratio of PANI/GO was increased to 9. These results indicate that higher PANI content in PANI/graphene composites does not bring in additional capacitance. Based on the results, the mass ratio of PANI/GO = 7 was adopted to study the reactions and interactions for the composites in this work.

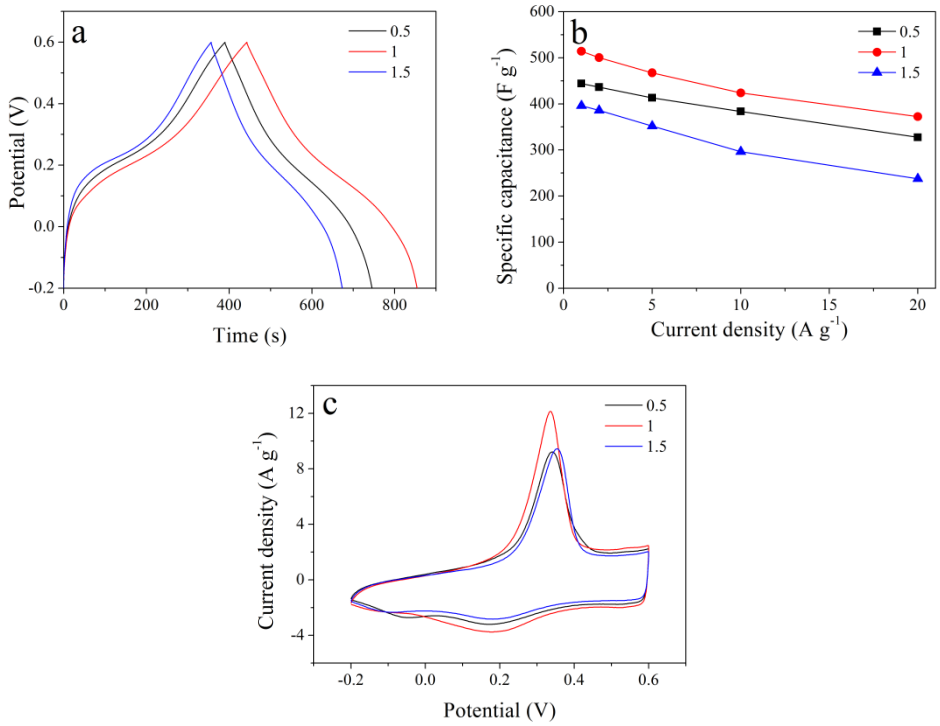

Fig. S13 The samples for different mass rates (0.5, 1 and 1.5) of mPD in GMPHs: (a) The charge/discharge curves at current density of 1 A g^{-1}; (b) Specific capacitance at different current densities; (c) The CV curves at the scan rate of 5 mV s^{-1}.

Fig. S14 Schematic structure of the solid-state supercapacitor.

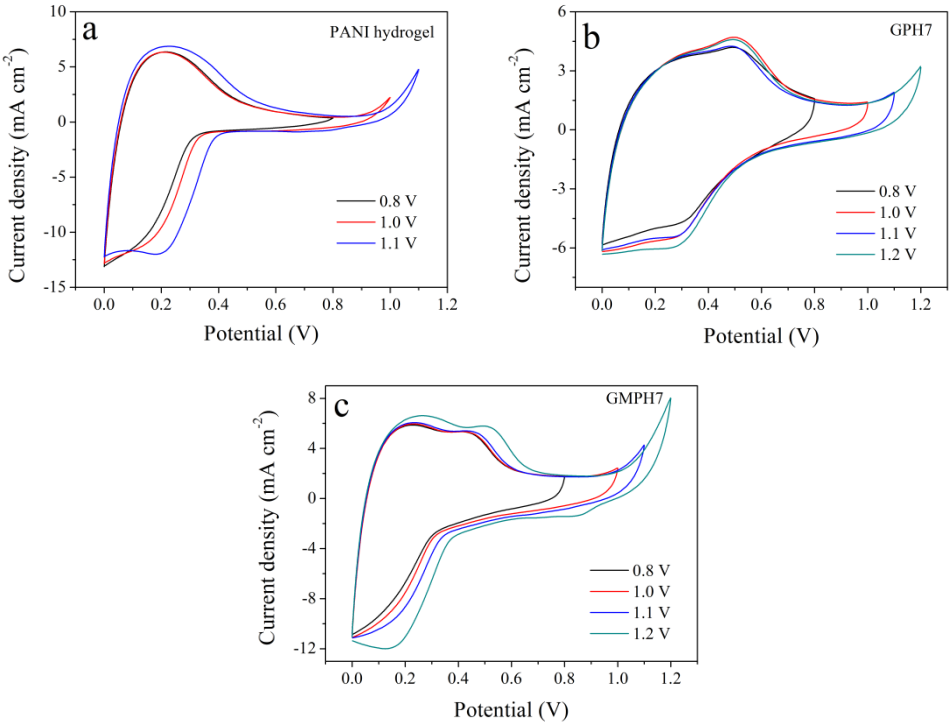

Fig. S15 The CV curves of (a) PANI hydrogel, (b) GPH7 and (c) GMPH7 under different potential range at a scan rate of 10 mV s^{-1}.

It can be seen that the CV curve of PANI hydrogel exhibit a certain degree of deformation under the potential range from 0–1.0 V and 0–1.1 V, which indicates that the potential range of 0–0.8 V is suitable for PANI hydrogel. However, GPH7 and GMPH7 display expanded potential range from 0 to 1.0 V.

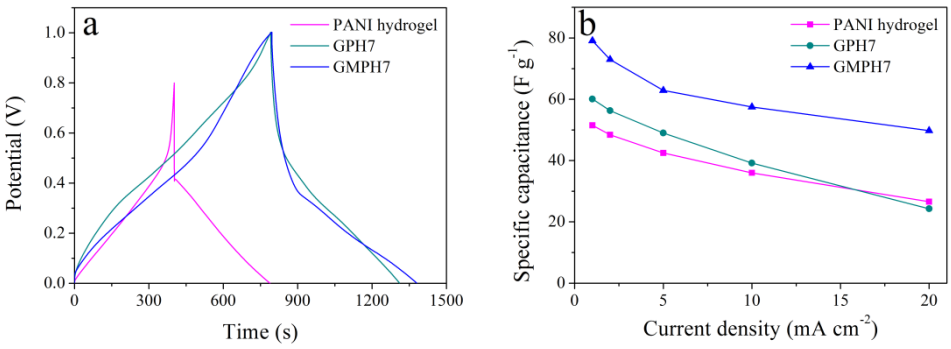

Fig. S16 (a) GCD curves at the current density of 1 mA cm^{-2}, and (b) the gravimetric specific capacitance against various current densities of PANI hydrogel, GPH7 and GMPH7 supercapacitors.

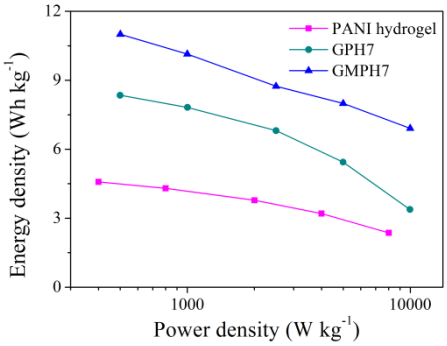

Fig. S17 Ragone plots of gravimetric energy density and power density of PANI hydrogel, GPH7 and GMPH7.

Table S1 The component mass loading in as-prepared samples based on the weight analysis.

Samples	Mass (g)	rGO mass loading (%)	Modified rGO mass loading (%)	PANI mass loading (%)
GPH7	0.153	9.2	--	90.8
GMPH7	0.167	--	16.8	83.2

Table S2 Elemental Composition of XPS analysis for PANI hydrogel, GPH7, GMPH7 and GH.

Samples	C (at.%)	O (at.%)	N (at.%)	S (at.%)
PANI hydrogel	81.91	5.29	12.26	0.54
GPH7	82.97	7.35	9.38	0.30
GMPH7	82.4	6.51	10.82	0.27
GH	85.61	14.39	—	—

Table S3 Relative ratio (at.%) of different carbon chemical bonds in the PANI hydrogel, GPH7, GMPH7 and GH obtained from XPS spectra.

Samples	C–C/C=C	C–N	C–O	C=N	C=O	the ratio of C=N to C–N
PANI hydrogel	47.8	36.6	—	15.6	—	42.6
GPH7	50.4	24.8	7.6	9.7	7.5	39.1
GMPH7	64.7	19.4	5.9	7.4	2.6	38.1
GH	59.0	—	18.8	12.0(O–C=O)	10.2	—

Table S4 Relative ratio (at.%) of different nitrogen chemical bonds in the PANI hydrogel, GPH7 and GMPH7 obtained from XPS spectra.

Samples	=N–	Pyridinic-N	–NH–	N^+	cyclic-N
PANI hydrogel	12.3	—	68.7	9.8	9.2
GPH7	11.3	—	68.7	7.8	12.2
GMPH7	18.3	4.2	61.4	7.3	8.8

Table S5 Electrochemical performance comparison of reported PANI and graphene/PANI composite electrodes based on three-electrode and/or two-electrode system.

samples	Current	C_s (F g^{-1})	Cycle	Method	Collector	Ref.
PANI hydrogel [a]		**325.3**	**78.9%, 1000**			**This work**
GPH7 [a]	**1 A g^{-1}**	**375.3**	**84.7%, 1000**	**Hydrothermal**	**Stainless steel**	
GMPH7 [a]		**514.3**	**87.1%, 1000**			
PPH [a]	1 A g^{-1}	806	86%, 1000	chemical crosslink	Carbon cloth	[S1]
Flexible graphene/PANI [a]	1 mV s^{-1} [c]	1126	84%, 1000	In-situ	Coat stainless steel	[S2]
PANI-graphene (PAFG) [a]	1 A g^{-1}	1295	88%,1500	In-situ chemical	Glassy carbon	[S3]
PNGH [a]	1 A g^{-1}	610	94.4%,1000	hydrothermal	Stainless steel	[S4]
PANI-CCG films [b]	5 A g^{-1}	450	85%,5000	In-situ	Platinum foils	[S5]
PANI hydrogel [a]	0.5 A g^{-1}	480	83%,1000	PA crosslink	Carbon cloth	[S6]
PANI-SA hydrogel [a]	0.5 A g^{-1}	252	71%,1000	In-situ	Drop stainless	[S7]
PANI hydrogel [a]	1 A g^{-1}	750	--	Self-crosslink	Carbon film	[S8]
RGO/PANI film [b]	0.5 A g^{-1}	385	88%,5000	Template situ	Gold foils	[S9]
PANI-GO [b]	0.5 A g^{-1}	555	92%,2000	In-situ	Gold grid	[S10]
GNS/PANi hydrogel [a]	2 A g^{-1}	334	52%,5000	In-situ assembled	Foamed nickel	[S11]
PANI@OGH film [b]	2 A g^{-1}	530	93%,10000	In-situ in OGH film	Pt foils	[S12]
PANI/GNs [a]	0.2 A g^{-1}	330	--	In-situ, reduced	Carbon black	[S13]
PAG80 [a]	0.1 A g^{-1}	480	--	In-situ	Glassy carbon	[S14]
PANI/GMS [b]	0.5 A g^{-1}	261	87.4%,10000	In-situ	Cast stainless-steel	[S15]
GQD-PANI [a]	1 A g^{-1}	1044	80.1%,3000	Reduced, in-situ	Glassy carbon	[S16]
PANI/graphene film [b]	0.5 A g^{-1}	384	84%,1000	In-situ electrophoretic	Nickel alloy plate	[S17]
GPN2 [a]	1 A g^{-1}	561.7	93.2%,1000	electrodeposition	--	[S18]

Graphene-PANI paper [a]	1 A g^{-1}	763	82%,1000	electropolymerization	--	[S19]
RGO/CNT/PANI papers [a]	0.2 A g^{-1}	257	--	electropolymerization	Gold	[S20]
GO/PANI [a]	1 A g^{-1}	1095	91.1%,1000	Interfacial electrochemical polymerization	Stainless steel	[S21]
rGO/PANI-NFs Hydrogel [b]	1 A g^{-1}	475	86%,1000	Hydrothermal	Stainless steel	[S22]
rGO/PANI films [a]	1 A g^{-1}	1182	108%,10000	Hydrothermal	Platinum plate	[S23]
PANi/graphene hydrogel [a]	0.4 A g^{-1}	223.82	87.5%,5000	Heat	Pt foil	[S24]
PANi-g-rGO [a]		250		In-situ graft	Glassy carbon	[S25]
grafted PANI/GO [a]	1 A g^{-1}	442	83%,2000	In-situ graft	Coated Pt foils	[S26]

[a] In a three-electrode system; [b] In a two-electrode system; [c] scan rate.

Table S6 The conductivity of as-prepared PANI hydrogel, GPH7 and GMPH7.

Samples	PANI hydrogel	GPH7	GMPH7
Conductivity (S cm^{-1})	0.064	0.177	0.123

Table S7 Performance comparison of the solid-state supercapacitor based on PANI and carbon/PANI.

Sample	**C_a (mF cm^{-2})**	**C_g (F g^{-1})**	**E_a (μWh cm^{-2})**	**E_g (Wh g^{-1})**	**Ref.**
PANI hydrogel/GPH7/GMPH7	**484/519.2/584.7, 1 mA cm^{-2}**	**51.5/60.1/79.1**	**42.96/60.9/81.28**	**4.58/8.35/11**	**This work**
PPH-5	420, 0.25 A g^{-1}	210	37.3	18.7	[S27]
3D-G/PANI	720, 1 A g^{-1}	122	64	10.9	[S28]
PANI nanotube	237.5, 10 mV s^{-1}	--	--	--	[S29]
PPH	306, 0.25 A g^{-1}	153	27.2	13.6	[S1]
PANI/AC device	522, 1 A g^{-1}	--	185	--	[S30]
PANI/CNT	422	103.4	--	--	[S31]
CNT@PANI film	573, 10 mV s^{-1}	--	50.98	--	[S32]
CNT/PANI hydrogel film	184.6, 1 mA cm^{-2}	--	--	--	[S33]
HGC-PANI-r	453, 5 mV s^{-1}	--	--	--	[S34]

Supplementary References

[S1] W. Li, F. Gao, X. Wang, N. Zhang and M. Ma. *Angew. Chem. Int. Ed.*, **2016**, *55*, 9196-9201.

[S2] H. Wang, Q. Hao, X. Yang, L. Lu and X. Wang. *Nanoscale*, **2010**, *2*, 2164-2170.

[S3] Y. Liu, Y. Ma, S. Guang, F. Ke and H. Xu. *Carbon*, **2015**, *83*, 79-89.

[S4] J. Luo, W. Zhong, Y. Zou, C. Xiong and W. Yang. *J. Power Sources*, **2016**, *319*, 73-81.

[S5] Y. Wang, X. Yang, A. G. Pandolfo, J. Ding and D. Li. *Adv. Energy Mater.*, **2016**, *6*, 1600185.

[S6] L. Pan, G. Yu, D. Zhai, H. R. Lee, W. Zhao, N. Liu, H. Wang, B. C. Tee, Y. Shi, Y. Cui and Z. Bao. *Proc. Natl. Acad. Sci. U.S.A.*, **2012**, *109*, 9287-9292.

[S7] H. Huang, X. Zeng, W. Li, H. Wang, Q. Wang and Y. Yang. *J. Mater. Chem. A*, **2014**, *2*, 16516-16522.

[S8] H. Guo, W. He, Y. Lu and X. Zhang. *Carbon*, **2015**, *92*, 133-141.

[S9] Y. Meng, K. Wang, Y. Zhang and Z. Wei. *Adv. Mater.*, **2013**, *25*, 6985-6990.

[S10] J. Xu, K. Wang, S.-Z. Zu, B.-H. Han and Z. Wei. *ACS Nano*, **2010**, *4*, 5019-5026.

[S11] Z. Tai, X. Yan and Q. Xue. *J. Electrochem. Soc.*, **2012**, ***159***, A1702-A1709.

[S12] Y. Wang, X. Yang, L. Qiu and D. Li. *Energy Environ. Sci.*, **2013**, *6*, 477-481.

[S13] C. Pan, H. Gu and L. Dong. *J. Power Sources*, **2016**, *303*, 175-181.

[S14] K. Zhang, L. L. Zhang, X. S. Zhao and J. Wu. *Chem. Mater.*, **2010**, *22*, 1392-1401.

[S15] H. Cao, X. Zhou, Y. Zhang, L. Chen and Z. Liu. *J. Power Sources*, **2013**, *243*, 715-720.

[S16] S. Mondal, U. Rana and S. Malik. *Chem. Commun.*, **2015**, *51*, 12365-12368.

[S17] Z. Tong, Y. Yang, J. Wang, J. Zhao, B.-L. Su and Y. Li. *J. Mater. Chem. A*, **2014**, *2*, 4642-4651.

[S18] M. Yu, Y. Ma, J. Liu and S. Li. *Carbon*, **2015**, *87*, 98-105.

[S19] H.-P. Cong, X.-C. Ren, P. Wang and S.-H. Yu. *Energy Environ. Sci.*, **2013**, *6*, 1185-1191.

[S20] Z.-D. Huang, R. Liang, B. Zhang, Y.-B. He and J.-K. Kim. *Compos. Sci. Technol.*, **2013**, *88*, 126-133.

[S21] D. Li, Y. Li, Y. Feng, W. Hu and W. Feng. *J. Mater. Chem. A*, **2015**, *3*, 2135-2143.

[S22] Z. Niu, L. Liu, L. Zhang, Q. Shao, W. Zhou, X. Chen and S. Xie. *Adv. Mater.*, **2014**, *26*, 3681-3687.

[S23] L. Zhang, D. Huang, N. Hu, C. Yang, M. Li, H. Wei, Z. Yang, Y. Su and Y. Zhang. *J. Power Sources*, **2017**, *342*, 1-8.

[S24] M. Moussa, Z. Zhao, M. F. El-Kady, H. Liu, A. Michelmore, N. Kawashima, P. Majewski and J. Ma. *J. Mater. Chem. A*, **2015**, *3*, 15668-15674.

[S25] N. A. Kumar, H.-J. Choi, Y. R. Shin, D. W. Chang, L. Dai and J.-B. Baek. *ACS Nano*, **2012**, *6*, 1715-1723.

[S26] Z.-F. Li, H. Zhang, Q. Liu, Y. Liu, L. Stanciu and J. Xie. *Carbon*, **2014**, *71*, 257-267.

[S27] W. Li, H. Lu, N. Zhang and M. Ma. *ACS Appl. Mater. Interfaces*, **2017**, *9*, 20142-20149.

[S28] K. Li, J. Liu, Y. Huang, F. Bu and Y. Xu. *J. Mater. Chem. A*, **2017**, *5*, 5466-5474.

[S29] H. Li, J. Song, L. Wang, X. Feng, R. Liu, W. Zeng, Z. Huang, Y. Ma and L. Wang. *Nanoscale*, **2017**, *9*, 193-200.

[S30] H. Heydari and M. B. Gholivand. *New J. Chem.*, **2017**, *41*, 237-244.

[S31] R. Liu, C. Liu and S. Fan. *J. Mater. Chem. A*, **2017**, *5*, 23078-23084.

[S32] J. Yu, W. Lu, S. Pei, K. Gong, L. Wang, L. Meng, Y. Huang, J. P. Smith, K. S. Booksh, Q. Li, J.-H. Byun, Y. Oh, Y. Yan and T.-W. Chou. *ACS Nano*, **2016**, *10*, 5204-5211.

[S33] S. Zeng, H. Chen, F. Cai, Y. Kang, M. Chen and Q. Li. *J. Mater. Chem. A*, **2015**, *3*, 23864-23870.

[S34] Y. Qu, C. Lu, Y. Su, D. Cui, Y. He, C. Zhang, M. Cai, F. Zhang, X. Feng and X. Zhuang. *Carbon*,

2018, *127*, 77-84.